

Sensitivity of Information Rates of Matching Circuits for Antenna Arrays

Andrei Nedelcu and Gerhard Kramer

Department of Electrical and Computer Engineering

Technical University of Munich

Email: andrei.nedelcu@tum.de, gerhard.kramer@tum.de

Submitted to the 2016 ITG Workshop on Smart Antennas, November 3, 2015

Abstract—A sensitivity analysis is performed for information rates of decoupling receiver matching circuits for antenna arrays. The sensitivity is computed by varying the antenna spacing, the device tolerances, and the bandwidth. The information rates are considerably reduced at antenna spacings below one-quarter wavelength.

I. INTRODUCTION

Antenna arrays should be made compact to save space but antenna proximity causes coupling which may reduce information rates. Matching circuits placed at the transmitter and receiver antennas serve to de-couple the antennas, or even better to maximize the mutual information between the transmitted bits and the received signal after quantization. This paper investigates matching circuits for narrowband and broadband signals. Sections II and III review models and theory for single-input, single-output (SISO) and multiple-input, multiple-output (MIMO) systems, respectively. Section IV presents a sensitivity analysis, where the sensitivity is computed by varying the antenna spacing, the device tolerances, and the bandwidth. Section V concludes the paper.

II. SISO ANTENNA SYSTEMS

A. Amplifier Noise

Rothe and Dahlke [1] introduced a theory of noisy fourpoles to characterize their noise behavior. The equivalent Thévenin representation of a noisy fourpole is given in Figure 1. Following the notation in [2] we define

$$\beta = \mathbb{E}[|i_N|^2] = 4kT_0Wg_n \quad (1)$$

$$R_N = \sqrt{\frac{\mathbb{E}[|v_N|^2]}{\mathbb{E}[|i_N|^2]}} \quad (2)$$

$$\rho = \frac{\mathbb{E}[v_N i_N^*]}{\sqrt{\mathbb{E}[|i_N|^2]\mathbb{E}[|v_N|^2]}} \quad (3)$$

where β is the input-referenced noise current total power, k is Boltzmann's constant, T_0 is the environment equilibrium temperature, W is the bandwidth in which the system operates, g_n is the equivalent noise conductance of the amplifier, R_N is the equivalent noise resistance, and ρ is the correlation coefficient between the noise voltage and the noise current. The noise random variables i_N and v_N are modeled as zero mean Gaussian with variances β and βR_N^2 respectively. This is consistent with the noise parameter definitions from [1].

B. External Noise

Apart from the noise originating at the active elements (amplifiers) there is also noise at the antenna [3]. Let $\Re\{X\}$ and $\Im\{X\}$ be the real and imaginary parts of the variable X , respectively. Using the Rayleigh-Jeans approximation, the antenna noise source can be represented by an equivalent Thévenin voltage source with (see [3])

$$\mathbb{E}[|v_{SN}|^2] = 4kT_A W \Re\{Z_{AR}\} \quad (4)$$

where the antenna noise temperature T_A is the equivalent temperature of a resistor with resistance $\Re\{Z_{AR}\}$ required to produce the same noise power as the actual environment seen by the antenna.

C. Impedance Matching

Consider Figure 2 where the amplifier impedance matrix is

$$Z_{amp} = \begin{bmatrix} Z_{amp11} & Z_{amp12} \\ Z_{amp21} & Z_{amp22} \end{bmatrix} \quad (5)$$

and there is a *lossless* and *reciprocal* matching circuit

$$Z_M = \begin{bmatrix} Z_{M11} & Z_{M12} \\ Z_{M12} & Z_{M22} \end{bmatrix} = j \begin{bmatrix} X_{M11} & X_{M12} \\ X_{M12} & X_{M22} \end{bmatrix} \quad (6)$$

where the X_{Mab} are real numbers. Following the development and notation in [2, Sec. IV.B], the source impedance

$$Z_{out} = -\frac{Z_{M12}^2}{Z_{AR} + Z_{M11}} + Z_{M22} \quad (7)$$

should satisfy $Z_{out} = Z_{opt}$ where

$$Z_{opt} = R_N \left(\sqrt{1 - \Im\{\rho\}^2} + j\Im\{\rho\} \right). \quad (8)$$

This choice maximizes the SNR which becomes [2, eq. (78)]

$$\text{SNR} = \frac{\mathbb{E}[|v_S|^2]}{4kT_A W \Re\{Z_{AR}\} F} \quad (9)$$

where F is the noise figure (here defined with respect to T_A) given by [2, eq. (82)]

$$F = 1 + \frac{\beta R_N}{2kT_A W} \left(\sqrt{1 - \Im\{\rho\}^2} - \Re\{\rho\} \right). \quad (10)$$

There is a class of Z_M that satisfies the constraint (8). For example, a simple choice is $Z_{M11} = -j\Im\{Z_{AR}\}$ so that

$$Z_M = j \begin{bmatrix} -\Im\{Z_{AR}\} & \pm \sqrt{\Re\{Z_{AR}\}\Re\{Z_{opt}\}} \\ \pm \sqrt{\Re\{Z_{AR}\}\Re\{Z_{opt}\}} & \Im\{Z_{opt}\} \end{bmatrix}. \quad (11)$$

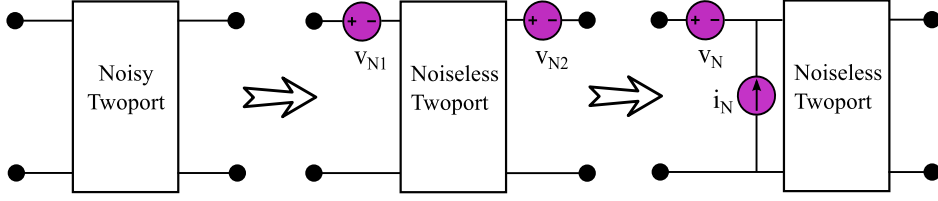


Fig. 1: Noisy fourpole models and equivalent circuits

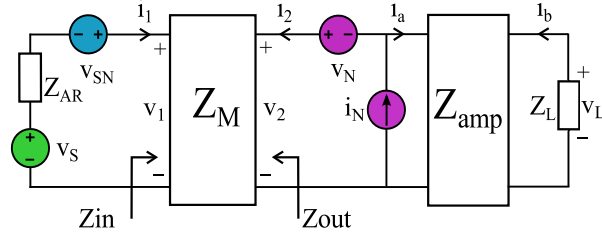


Fig. 2: Single antenna front-end receiver with impedance matching

III. MIMO ANTENNA SYSTEMS

A. System Model

The system model of Sec. II can be extended to MIMO systems (see, e.g., [2], [4]). Figure 3 shows a MIMO system with N antennas, N amplifiers, and a $2N \times 2N$ matching circuit (more generally, one could use $2N \times 2M$ matching circuits with $M \neq N$). Our focus will be on matching and we begin with a narrow-band assumption, i.e., the bandwidth is a small fraction of the carrier frequency. We will assume as in Sec. II that the matching networks are passive, lossless, and reciprocal. We consider the amplifiers to be operated in the linear regime.

B. Transmitter Equations

We assume that both the transmitter matching circuit and the antennas are lossless, i.e., $\mathbb{E}[\Re\{\mathbf{v}_{AT}^H \mathbf{i}_{AT}\}] = \mathbb{E}[\Re\{\mathbf{v}_T^H \mathbf{i}_T\}]$ where the vectors have length N . The transmit power is

$$\begin{aligned} \mathbb{E}[\Re\{\mathbf{v}_{AT}^H \mathbf{i}_{AT}\}] &= \mathbb{E}[\Re\{\mathbf{i}_{AT}^H \mathbf{Z}_{AT}^H \mathbf{i}_{AT}\}] \\ &= \mathbb{E}[\Re\{\mathbf{v}_G^H \mathbf{C}_T \mathbf{v}_G\}] \end{aligned} \quad (12)$$

where

$$\begin{aligned} \mathbf{C}_T &= (\mathbf{Z}_T + \mathbf{Z}_G)^{-H} \mathbf{Z}_{MT21}^H (\mathbf{Z}_{MT22} + \mathbf{Z}_{AT})^{-H} \mathbf{Z}_{AT}^H \\ &\quad (\mathbf{Z}_{MT22} + \mathbf{Z}_{AT})^{-1} \mathbf{Z}_{MT21} (\mathbf{Z}_T + \mathbf{Z}_G)^{-1} \end{aligned} \quad (13)$$

is the transmit coupling matrix. Relating the noiseless antenna input and output currents and voltages we have

$$\begin{bmatrix} \mathbf{v}_{AT} \\ \mathbf{v}_{AR} \end{bmatrix} = \begin{bmatrix} \mathbf{Z}_{AT} & \mathbf{Z}_{TR} \\ \mathbf{Z}_{RT} & \mathbf{Z}_{AR} \end{bmatrix} \begin{bmatrix} \mathbf{i}_{AT} \\ \mathbf{i}_{AR} \end{bmatrix} \quad (14)$$

where \mathbf{Z}_{AT} and \mathbf{Z}_{AR} are the transmit and receive array impedance matrices and \mathbf{Z}_{TR} and \mathbf{Z}_{RT} are the channel impedances from the transmitter to the receiver and from the receiver to the transmitter. Given the large separation that usually exists between terminals, the re-scattered power is

negligible and we can assume $\mathbf{Z}_{TR} \approx 0$. The resulting transfer matrix is

$$\mathbf{Z}_{TCR} = \begin{bmatrix} \mathbf{Z}_{AT} & \mathbf{0} \\ \mathbf{Z}_{RT} & \mathbf{Z}_{AR} \end{bmatrix}. \quad (15)$$

C. Channel Model and Fading

The physical channel \mathbf{Z}_{RT} is generally stochastic and can be modeled by methods presented in [5]. We use the widely known Kronecker model [5]. We compute [2, eq. (16)]

$$\mathbf{v}_L = \mathbf{C}_L (\mathbf{X} + \mathbf{Z}_R)^{-1} \mathbf{F}_R (\mathbf{H} \mathbf{v}_G + \mathbf{v}_{noise}) \quad (16)$$

where

$$\mathbf{H} = \mathbf{Z}_{RT} \mathbf{Z}_{TT} \quad (17)$$

$$\mathbf{v}_{noise} = \mathbf{v}_{SN} + \mathbf{F}_R^{-1} (\mathbf{Z}_R \mathbf{i}_N - \mathbf{v}_N) \quad (18)$$

with the component matrices [2, eq. (17)-(20)]

$$\mathbf{C}_L = \mathbf{Z}_L (\mathbf{Z}_L + \mathbf{Z}_{22amp})^{-1} \quad (19)$$

$$\mathbf{F}_R = \mathbf{Z}_{MR21} (\mathbf{Z}_{MR11} + \mathbf{Z}_{AR})^{-1} \quad (20)$$

$$\mathbf{Z}_R = \mathbf{Z}_{MR22} - \mathbf{F}_R \mathbf{Z}_{MR12} \quad (21)$$

$$\mathbf{X} = \mathbf{Z}_{11amp} - \mathbf{Z}_{12amp} (\mathbf{Z}_{22amp} + \mathbf{Z}_L)^{-1} \mathbf{Z}_{21amp} \quad (22)$$

$$\mathbf{Z}_{TT} = \mathbf{F}_T^T (\mathbf{Z}_T + \mathbf{Z}_G)^{-1} \quad (23)$$

$$\mathbf{F}_T = \mathbf{Z}_{MT12} (\mathbf{Z}_{MT22} + \mathbf{Z}_{AT})^{-1} \quad (24)$$

$$\mathbf{Z}_T = \mathbf{Z}_{MT11} - \mathbf{F}_T \mathbf{Z}_{MT21}. \quad (25)$$

We assume that \mathbf{F}_R in (20) is invertible. Observe from (16) that $\mathbf{C}_L (\mathbf{X} + \mathbf{Z}_R)^{-1} \mathbf{F}_R$ multiplies both the signal and noise and is invertible. We thus focus on the voltage signal

$$\hat{\mathbf{v}}_L = \mathbf{H} \mathbf{v}_G + \mathbf{v}_{noise}. \quad (26)$$

We will restrict attention to passive, lossless, and reciprocal matching networks, i.e., \mathbf{Z}_{MR} has imaginary entries and $\mathbf{Z}_{MR} = -\mathbf{Z}_{MR}^H$. The matching network impedance matrix thus has the form

$$\mathbf{Z}_{MR} = \begin{bmatrix} \mathbf{Z}_{MR11} & \mathbf{Z}_{MR12} \\ \mathbf{Z}_{MR12}^T & \mathbf{Z}_{MR22} \end{bmatrix} = j \begin{bmatrix} \mathbf{X}_{MR11} & \mathbf{X}_{MR12} \\ \mathbf{X}_{MR12}^T & \mathbf{X}_{MR22} \end{bmatrix} \quad (27)$$

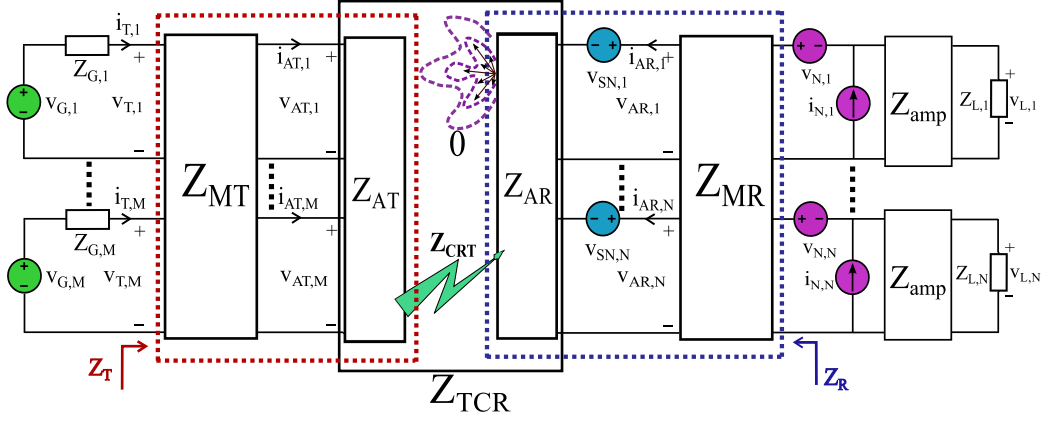


Fig. 3: MIMO front-end transceiver with matching

where the \mathbf{X}_{MRab} are real matrices, and \mathbf{X}_{MR11} and \mathbf{X}_{MR22} are symmetric.

D. Amplifier Noise

The voltage and current noise sources are modeled by Gaussian random variables with zero mean and second order statistics given by [2, eq. (10)]

$$\mathbb{E}[\mathbf{i}_N \mathbf{i}_N^H] = \beta \mathbf{I} \quad (28)$$

$$\mathbb{E}[\mathbf{v}_N \mathbf{v}_N^H] = \beta R_N^2 \mathbf{I} \quad (29)$$

$$\mathbb{E}[\mathbf{v}_N \mathbf{i}_N^H] = \rho \beta R_N \mathbf{I}. \quad (30)$$

Diagonal noise covariance matrices [2] [4] [6] are reasonable if the amplifiers are well isolated on a chip.

E. External Noise

Suppose the background noise is due to randomly polarized planar waves propagating from all angles uniformly. We follow the development of [2] to write the open circuit noise voltage covariance as

$$\mathbb{E}[\mathbf{v}_{SN} \mathbf{v}_{SN}^H] = 4kWT_A \Re\{\mathbf{Z}_{AR}\} \quad (31)$$

where $\Re\{\mathbf{Z}_{AR}\}$ is positive semidefinite. If there are additional losses, the antenna impedance may be augmented by a real matrix \mathbf{R}_{AL} to obtain

$$\mathbb{E}[\mathbf{v}_{SN} \mathbf{v}_{SN}^H] = 4kWT_A \Re\{\mathbf{Z}_{AR}\} + 4kWT_{AL} \mathbf{R}_{AL}. \quad (32)$$

F. Gaussian Channel MIMO Mutual Information

Suppose the voltages are sampled once per symbol (recall that we are working with a narrowband assumption) and that we abuse notation and represent the samples by \mathbf{v}_G and $\hat{\mathbf{v}}_L$. The mutual information between source and load voltages given that the receiver has perfect channel state information (CSI) is

$$\begin{aligned} I(\mathbf{v}_G; \hat{\mathbf{v}}_L) &= h(\hat{\mathbf{v}}_L) - \log_2((\pi e)^N \det(\mathbf{C}_{noise})) \\ &\leq \log_2 \det(\mathbf{I} + \mathbf{C}_{noise}^{-1} \mathbf{Z}_{RT} \mathbf{Z}_{TT} \mathbf{C}_{vG} \mathbf{Z}_{TT}^H \mathbf{Z}_{RT}^H) \end{aligned} \quad (33)$$

where

$$\begin{aligned} \mathbf{C}_{noise} &= 4kT_A W \Re\{\mathbf{Z}_{AR}\} \\ &+ \beta \mathbf{F}_R^{-1} (\mathbf{Z}_R \mathbf{Z}_R^H + R_N^2 \mathbf{I} - 2R_N \Re\{\rho \mathbf{Z}_R^H\}) \mathbf{F}_R^{-H}. \end{aligned} \quad (34)$$

We have equality in (33) if and only if \mathbf{v}_G is a Gaussian distributed vector.

G. Capacity

The capacity is obtained by maximizing the mutual information over the transmitter and receiver matching networks, subject to the power constraints

$$\text{Tr}\{\mathbf{C}_{vG}\} \leq P_{av} \quad (35)$$

$$\mathbb{E}\{\Re\{\mathbf{v}_G^H \mathbf{C}_T \mathbf{v}_G\}\} \leq P_{rad}. \quad (36)$$

The constraint (35) limits the total supplied power, which for decoupled antennas with perfect matching also constrains the radiated power. However, in a coupled MIMO system the supplied power is not necessarily the same as the radiated power, which is the quantity constrained by regulatory bodies. This has been highlighted in [6] that introduced the radiated power constraint (36).

To determine the optimal receiver matching network we use the following theorem whose proof is outlined in the Appendix. Consider Hermitian matrices \mathbf{A}, \mathbf{B} . We write $\mathbf{A} \succeq \mathbf{B}$ if the matrix $\mathbf{A} - \mathbf{B}$ is positive semidefinite and $\mathbf{A} \succ \mathbf{B}$ if $\mathbf{A} - \mathbf{B}$ is positive definite.

Theorem 1: For a fixed $\mathbf{M} \succeq \mathbf{0}$ and $\mathbf{C}_1, \mathbf{C}_2 \succ \mathbf{0}$ we have

$$\mathbf{C}_1 \succ \mathbf{C}_2 \Rightarrow \log_2 \det(\mathbf{I} + \mathbf{C}_2^{-1} \mathbf{M}) > \log_2 \det(\mathbf{I} + \mathbf{C}_1^{-1} \mathbf{M}).$$

We now rewrite \mathbf{C}_{noise} in (34) as

$$\begin{aligned} 4kT_A W \Re\{\mathbf{Z}_{AR}\} &+ \mathbf{F}_R^{-1} \beta ((\mathbf{Z}_R - \mathbf{Z}_{opt} \mathbf{I})(\mathbf{Z}_R - \mathbf{Z}_{opt} \mathbf{I})^H \\ &- 2R_N \Re\{\rho \mathbf{Z}_R^H\} + 2\Re\{\mathbf{Z}_{opt} \mathbf{Z}_R^H\}) \mathbf{F}_R^{-H}. \end{aligned} \quad (37)$$

From the lossless property of the matching network, namely that the available power at the input and output of the matching network is conserved, we compute

$$\Re\{\mathbf{Z}_R\} = \mathbf{F}_R \Re\{\mathbf{Z}_{AR}\} \mathbf{F}_R^H. \quad (38)$$

Thus, from (37) we have

$$\mathbf{C}_{noise} \succeq 4kT_A W \Re\{\mathbf{Z}_{AR}\} F \quad (39)$$

where F is the noise figure (10). We have equality in (39) if $\mathbf{Z}_R = Z_{opt}\mathbf{I}$, and there is a class of \mathbf{Z}_{MR} that accomplishes this. A simple approach (see [2], [4], but also [7]) is to choose $\mathbf{Z}_{MR11} = -j\Im\{\mathbf{Z}_{AR}\}$ and

$$\mathbf{Z}_{MR} = j \begin{bmatrix} -\Im\{\mathbf{Z}_{AR}\} & (\Re\{\mathbf{Z}_{AR}\}\Re\{Z_{opt}\})^{1/2} \\ (\Re\{\mathbf{Z}_{AR}\}\Re\{Z_{opt}\})^{1/2} & \Im\{Z_{opt}\}\mathbf{I} \end{bmatrix}. \quad (40)$$

IV. SENSITIVITY ANALYSIS

We next evaluate the sensitivity of the above matching circuits by varying the device tolerances, the bandwidth, and the antenna spacing.

1) *Antennas*: Suppose both the transmit and receive arrays are uniform linear arrays (ULA) with half-wavelength (resonant) dipoles with center feed oriented in parallel to each other. Closed form expressions exist for the self and mutual impedance of very thin wire dipoles [8], however no such expressions exist for radiation patterns. This motivates evaluating the antenna array impedance matrix and patterns using a numerical method of moments (MoM) provided by the Antenna Toolbox in Matlab and benchmarked against 4nec2 [9] software. We use dipoles of length $\lambda/2$ and width $\lambda/100$ separated by spacings no smaller than 0.05λ . We evaluate the antenna properties at the center frequency $f_c = 800\text{MHz}$.

2) *Noise Parameters*: We consider amplifiers with $R_N = 10\Omega$, $Z_{opt} = 56.74 + j10.66$, and minimum noise factor $F_{min} = 1.36\text{dB}$. These parameters are motivated by considering perfectly unilateral amplifiers with $Z_{amp12} = 0\Omega$, $|Z_{amp21}| \gg 1$, and $Z_{amp11} = Z_{opt}^*$, i.e., we consider

$$\mathbf{Z}_{amp} = \begin{bmatrix} Z_{opt}^* & 0 \\ Z_{amp21} & Z_{amp22} \end{bmatrix}. \quad (41)$$

Such models do not depart much from well designed catalog amplifiers used in [4] [6]. Note, however, that \mathbf{Z}_{amp} does not affect the capacity calculation.

3) *Achievable Rates*: We consider CSI at the receiver while the transmitter knows only the statistics of the channel. In this case isotropic diagonal power allocation $\mathbf{C}_{v_G} = \frac{P}{N}\mathbf{I}$, where P is the transmitted power and N is the number of transmit/receive antennas, is the best strategy [10].

For each antenna spacing we evaluate the rate by Monte Carlo simulation with 25000 channel realizations. We compare the optimal receive matching rates with:

- independent and identically distributed (iid) fading and noise; the fading is Rayleigh and flat, and the receiver noise is spatially white.
- self matching, i.e., the dipole antennas are matched to the optimal noise impedance of the amplifier so that

$$\mathbf{Z}_{MR, self, ab} = j \text{diag}(\mathbf{X}_{MRab}) \quad (42)$$

where $\text{diag}(\cdot)$ retains the diagonal of a matrix.

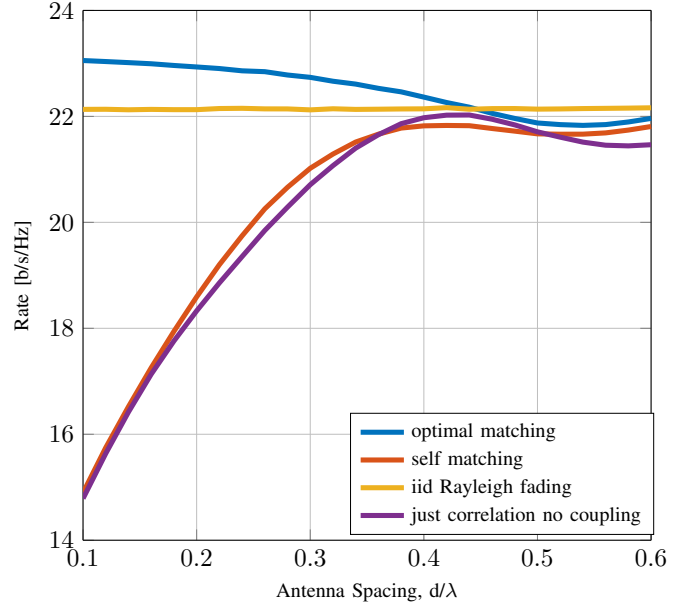


Fig. 4: Rates with receiver CSI vs. antenna spacing

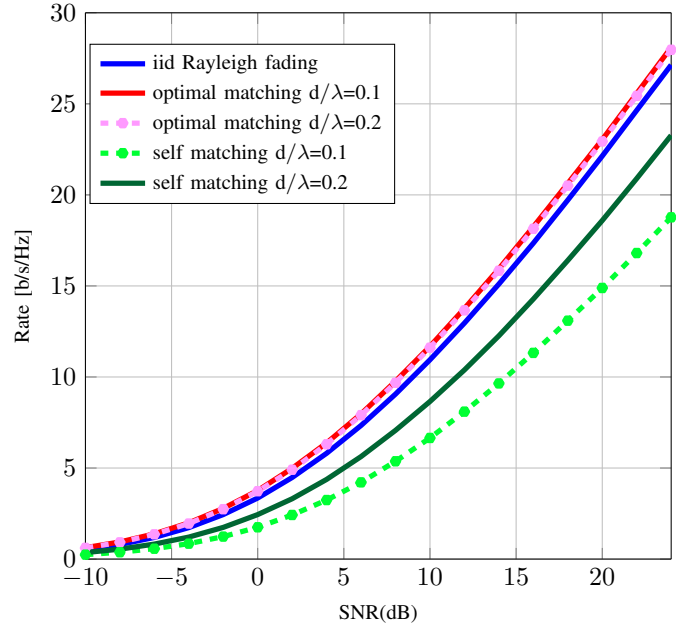


Fig. 5: Rates with receiver CSI vs. SNR

For fair comparison we scale the channel covariance matrices so that $\mathbb{E}\{\text{Tr}\{\mathbf{Z}_{RT}\mathbf{Z}_{RT}^H\}\} = N^2$. The SNR is defined with respect to the SISO SNR. We note that for uncoupled and uncorrelated MIMO RF chains the individual chain SNR is equal to our definition of the SISO SNR.

A. Antenna Spacing

We consider $N = 4$. Figure 4 shows the rate as a function of the spacing between antenna elements at the receive array for the cases of interest enumerated above. The SNR is fixed at 20dB. For small spacings the rates achieved by coupled dipoles

exceed the ones achieved with iid fading and noise. This is due to the increase of the power collection of the decoupled and matched array due to its larger effective aperture compared with the uncoupled array [11].

Figure 5 plots the rate vs. SNR for two antenna separations $d = 0.1\lambda$ and $d = 0.2\lambda$. At low SNR the gap between suboptimal and optimal matching is not significant and therefore tighter spacings can be used with suboptimal matching without large rate penalties. However, at high SNR the gap is significant. For example at a spacing of 0.1λ and a rate of 15 bits/s/Hz there is a SNR backoff of 7 dB as compared to optimal matching.

We remark that an optimal decoupling network is complex and may result in a large and bulky front-end. An optimal matching network has a complexity of $2N^2 + N$ network elements and requires connections between all pairs of antennas. Research into low complexity implementations of such networks is presented in [7] and references therein.

B. Device Variations

The receiver matching network was derived by maximizing the mutual information at one frequency. However, most applications require operating well over a large spectral range. In addition, realistic components will cause the entries of the matching network to differ from the desired ones for reasons such as losses, parasitic effects, availability of only a discrete set of nominal values (e.g. for lumped elements), fabrication tolerances, temperature and aging effects. We investigate the robustness of the matching network to device variations.

Figure 6 plots the average achievable rate as a function of antenna spacing at an SNR of 20dB. The tolerances have been chosen equal for all four component sub-matrices of \mathbf{Z}_{MR} . Here tolerance does not refer to the individual discrete inductor or capacitor tolerances, i.e., we do not consider particular realizations and topologies. We instead lump all the variations into a final variation of the chosen values. These final variations are uniformly distributed around the nominal value in the interval $[-tol, +tol]$. The averaging is done over 1000 realizations of the channel and over 1000 instances of the perturbed matching network. The standard deviation of the rate is represented by the vertical bars. We note that tolerance has significant impact at spacings below 0.25λ . At a tolerance level of 10%, placing antennas 0.2λ apart achieves the same average performance as 0.5λ . This means that a matching network lets one reduce the array aperture by a factor of 2.5.

C. Broadband Rates

Figure 7 shows the rate as a function of antenna spacing at double sided bandwidths of 1%, 5% and 10% of the carrier frequency f_c . The receiver optimal matching network is computed for the parameters found at the central frequency. The bandwidth is divided in $K = 200$ equally spaced bands.

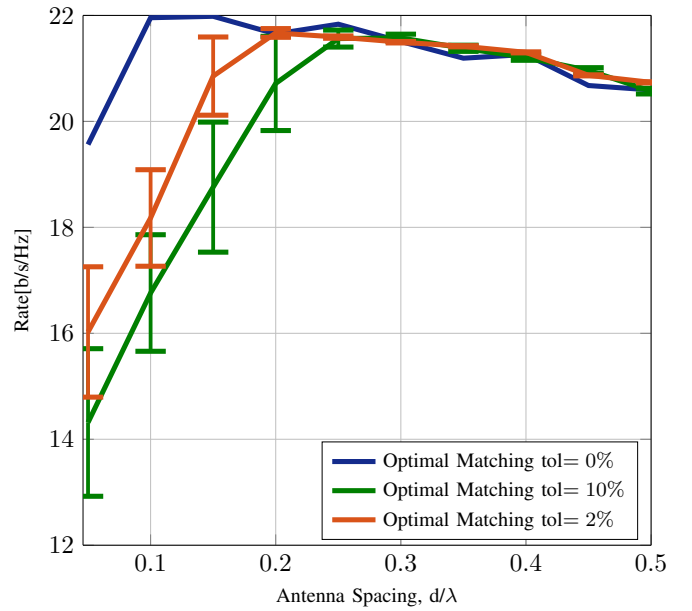


Fig. 6: Rates vs. antenna spacing with element tolerances

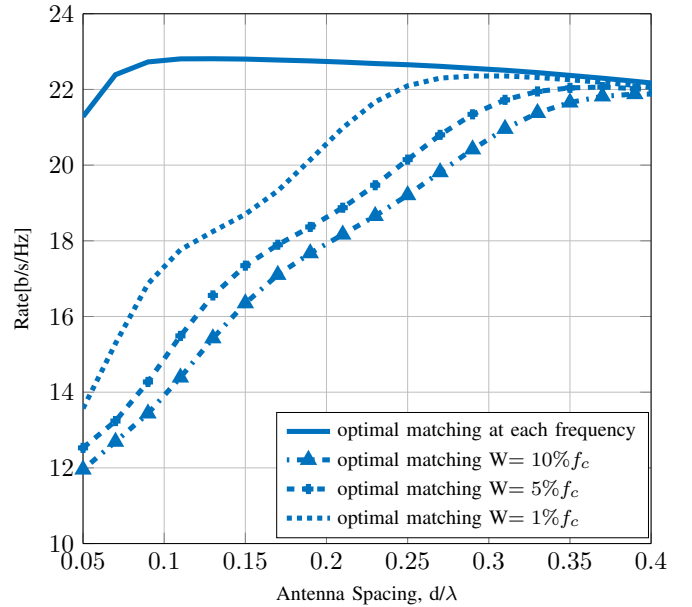


Fig. 7: Rates vs. antenna spacing with varying bandwidth

The mid-frequency in each band will be denoted as f_k . Therefore the total rate per unit of bandwidth is

$$I(\mathbf{v}_G; \hat{\mathbf{v}}_L) = \frac{1}{K} \sum_{k=1}^K \log_2 \det (\mathbf{I} + \mathbf{C}_{noise, f_k}^{-1} \mathbf{Z}_{RT, f_k} \mathbf{Z}_{TT, f_k} \mathbf{C}_{v_G} \mathbf{Z}_{TT, f_k}^H \mathbf{Z}_{RT, f_k}^H) \quad (43)$$

where all other channel and network parameters except the matching network are evaluated at the mid-frequencies f_k over which the summation is done. The plot shows that the optimal matching network is highly frequency selective. This motivates

the need for a broadband solution for matching networks for coupled MIMO systems, which has been studied in [12], [13], [14], [15], [16] for example.

V. CONCLUSION

The sensitivity of information rates of receiver matching circuits was analyzed with respect to the antenna spacing, the device tolerances, and the bandwidth. The analysis shows that the information rates are considerably reduced at antenna spacings below one-quarter wavelength. The results motivate developing matching circuits that are robust to uncertainties in the device parameters, and that give good broadband performance.

APPENDIX

Combining the following Propositions proves Theorem 1.

Proposition 1: If $\mathbf{A} \succeq \mathbf{B}$ then for every operator \mathbf{X} we have $\mathbf{X}^* \mathbf{A} \mathbf{X} \succeq \mathbf{X}^* \mathbf{B} \mathbf{X}$.

Proposition 2 (Corollary 7.7.4 in [17]): If $\mathbf{A} \succeq \mathbf{B} \succ \mathbf{0}$ then $\mathbf{B}^{-1} \succeq \mathbf{A}^{-1}$.

Proposition 3 (Corollary 7.7.4 (b) in [17]): If $\mathbf{A} \succeq \mathbf{B} \succ \mathbf{0}$ then $\det \mathbf{A} \succeq \det \mathbf{B}$.

Proposition 4: If $\mathbf{A} \succeq \mathbf{B}$ then $\mathbf{A} + \mathbf{I} \succeq \mathbf{B} + \mathbf{I}$.

Proposition 5: According to Theorem 7.2.6 in [17], for a positive semidefinite matrix \mathbf{M} there is a positive semidefinite matrix \mathbf{D} such that $\mathbf{D}^2 = \mathbf{M}$ and \mathbf{D} can be denoted as $\mathbf{M}^{1/2}$. Then we have the following identity:

$$\det(\mathbf{I} + \mathbf{C}^{-1} \mathbf{M}) = \det(\mathbf{I} + \mathbf{M}^{1/2} \mathbf{C}^{-1} \mathbf{M}^{1/2}). \quad (44)$$

REFERENCES

- [1] H. Rothe and W. Dahlke, "Theory of noisy fourpoles," *Proc. IRE*, vol. 44, pp. 811–818, June 1956.
- [2] M.T. Ivrlac and J.A. Nassek, "Toward a circuit theory of communication," *IEEE Trans. Circuits Syst. I*, vol. 57, no. 7, pp. 1663–1683, July 2010.
- [3] D.M. Pozar, *Microwave engineering*, Wiley, 2009.
- [4] C. P. Domizioli and B. L. Hughes, "Front-end design for compact MIMO receivers: a communication theory perspective," *IEEE Trans. Commun.*, vol. 60, no. 10, pp. 2938–2949, 2012.
- [5] C. Oestges and B. Clerckx, *MIMO Wireless Communications: From Real-world Propagation to Space-Time Code Design*, Academic Press, 2010.
- [6] M. L. Morris and M. Jensen, "Network model for MIMO systems with coupled antennas and noisy amplifiers," *IEEE Trans. Antennas Propag.*, vol. 53, no. 1, pp. 545–552, 2005.
- [7] D. Nie, B. M. Hochwald, and E. Stauffer, "Systematic design of large-scale multiport decoupling networks," *IEEE Trans. Circuits Syst. I*, vol. 61, no. 7, 2014.
- [8] C. A. Balanis, *Antenna theory: Analysis and Design*, vol. 1, Wiley, 2005.
- [9] A. Voors, "4nec2, NEC based antenna modeler and optimizer," 2015, [accessed 4-October-2015].
- [10] I. E. Telatar, "Capacity of multi-antenna Gaussian channels," *Eur. Trans. Telecommun.*, vol. 10, no. 6, pp. 585–595, 1999.
- [11] J. W. Wallace and M. Jensen, "Mutual coupling in MIMO wireless systems: a rigorous network theory analysis," *IEEE Trans. Wireless Commun.*, vol. 3, no. 4, 2004.
- [12] R. M. Fano, "Theoretical limitations on the broadband matching of arbitrary impedances," *J. Franklin Institute*, vol. 249, no. 1, pp. 57–83, 1950.
- [13] W.-K. Chen, "Mathematical theory of broadband matching of multiport networks," *J. Franklin Institute*, vol. 326, no. 5, pp. 737–747, 1989.

- [14] P. S. Taluja and B. L. Hughes, "Bandwidth limitations and broadband matching for coupled multi-antenna systems," in *Global Telecommun. Conf., 2011 IEEE*. IEEE, 2011, pp. 1–6.
- [15] L. Kundu and B. L. Hughes, "The impact of frequency-selective matching on the capacity of compact MIMO systems," in *2014 IEEE Int. Conf. Commun.*, 2014, pp. 2215–2220.
- [16] D. Nie and B. M. Hochwald, "Broadband matching bounds for coupled loads," *IEEE Trans. Circuits Syst. I*, vol. 62, no. 4, 2015.
- [17] R.G. Horn and C.R. Johnson, *Matrix Analysis*, Cambridge, 1985.